Approaches to radar reflectivity bias correction to improve rainfall estimation in Korea

C.-H. You[1], M.-Y. Kang[2], D.-I. Lee[1,2], and J.-T., Lee[2]

[1] {Atmospheric Environmental Research Institute, Pukyong National University, Busan, South Korea}

[2] {Department of Environmental Atmospheric Sciences, Pukyong National University, Busan, South Korea}

Correspondence to: D.-I. Lee (leedi@pknu.ac.kr)

Abstract

Three methods for determining the reflectivity bias of single polarization radar using dual polarization radar reflectivity and disdrometer data (i.e., the equidistance line, overlapping area, and disdrometer methods) are proposed and evaluated for two low-pressure rainfall events that occurred over the Korean Peninsula on 25 August 2014 and 8 September 2012. Single polarization radar reflectivity was underestimated by more than 12 dB and 7 dB in the two rain events, respectively. All methods improved the accuracy of rainfall estimation, except for one case where DSDs were not observed, as the precipitation system did not pass through the disdrometer location. The use of these bias correction methods reduced the RMSE by as much as 50%. Overall, the most accurate rainfall estimates were obtained using the overlapping area method to correct radar reflectivity.

1 Introduction

Radar is a useful remote sensing instrument for measuring rainfall amount, due to its relatively high resolution in both space and time. Areal rainfall rate is not measured directly, but must be derived from radar reflectivity. This estimation of radar rainfall is based on the relationship between reflectivity (Z) and rainfall rate (R), known as the Z–R relation (R(Z)). Experimentally measured drop size distributions (DSDs) have been used extensively to obtain both radar reflectivity and rainfall rate (Compos and Zawadzki, 2000; Jang et al., 2004; You et al., 2004).

There is no unique R(Z), since DSDs can be varied storm to storm and even within a single storm (Battan 1973; You et al., 2010).

However, radar rainfall estimation is complicated by a number of uncertainties including hardware calibration, partial beam filling, rain attenuation, brightband, and non-weather echoes (Wilson and Brandes, 1979; Austin, 1987). The correction of bias in Z caused by hardware calibration error is difficult to achieve using single polarimetric radar (SPOL) alone. Polarimetric radar (DPOL) provides a new method for the absolute calibration of reflectivity, which has been a longstanding problem with single polarization radar data. The method is based on the assumptions that Z, differential reflectivity (Z_{DR}), and specific differential phase (K_{DP}) are independent of each other, and that Z can be estimated from Z_{DR} and K_{DP}, which are insensitive to radar miscalibration (Gorgucci et al., 1992, 1999; Goddard et al., 1994; Scarchilli et al., 1996; Vivekanandan et al., 1999).

The Korea Meteorological Administration (KMA) is in the process of replacing Doppler radars with S-band DPOLs (to be completed by 2019), and Ministry of Land, Infrastructure and Transport (MoLIT) has installed four S-band DPOLs for operational use since 2009. Until the DPOL installation is complete, it is necessary to use a combination of SPOLs and DPOLs to produce rainfall mosaics covering the whole Korean Peninsula. To obtain more accurate mosaicked radar rainfall, SPOL reflectivity should be corrected using the reflectivity of DPOLs and other instruments such as disdrometer. Accurate SPOL reflectivity is also required for climatological analysis using radar rainfall.

This paper discusses three methods for reducing errors in SPOL reflectivity using DPOL and DSD measurements. In Section 2, the dataset used for the analysis is introduced, and three approaches to correcting SPOL reflectivity are described, along with methods for bias correction of DPOL reflectivity and Z_{DR}, and for validation. In Section 3, the results obtained using the three correction methods are compared with gauge measurements. Finally, we summarize the results and provide conclusions in Section 4.

2 Data

Rainfall data from rain gauges operated by the KMA were used to evaluate the accuracy of radar rainfall. Rain gauges located between 5 and 134 km from the radar were included in the analysis. Figure 1 shows the location of all instruments used in this study. The PARSIVEL

(PARticle SIze VELocity) disdrometer was installed ~9 km from PSN. PARSIVEL is a laser-optic system that measures 32 channels from 0.062 to 24.5 mm (for detailed specifications, see Loffler-Mang and Joss, 2000).

Data observed from PARSIVEL were regarded as unreliable and removed from the analysis in the case that any of the following conditions were met: 1 min rain rate was less than 0.1 mm h^{-1}; total number concentration from all channels was less than 10; drop numbers were recorded only in the lower 10 channels (1.187 mm for PARSIVEL); or drop numbers were recorded only in the lower 5 channels (0.562 mm for PARSIVEL) (You et al., 2015).

Radar data were recorded at PSN (Pusan radar) is located at coastal line and BSL (Bisalsan radar) is located 76.9 km away from PSN (Fig. 1), which were installed and are operated by KMA and MoLIT, respectively. The transmitted peak power of BSL is 750 kW, the beam width is 0.95 °, the frequency is 2.791 GHz, and the antenna is 1085 m above sea level. The polarimetric variables are estimated with a gate size of 0.125 km. The scan strategy consists of six elevation angles with a 2.5 min update interval. The transmitted peak power of PSN is 800 kW, the beam width is 1.0 degrees, the frequency is 2.712 GHz and the antenna is 547 m above sea level. The reflectivity is estimated with a gate size of 0.25 km. The PSN scan strategy consists of 13 elevation angles with a 10 min update interval. Radar variables at an elevation angle of 0.5 (1.8) degrees were extracted from the BSL (PSN) data every 10 mins, to match the time interval for this study. Non-meteorological targets were removed from the PSN data using the texture and vertical gradient of reflectivity, as proposed by Zhang et al. (2004). Polarimetric variables were subjected to quality control using a threshold of 15 degrees for the standard deviation of the differential phase shift (You et al., 2014).

The quality controlled Z_H, Z_{DR}, K_{DP} measured from BSL were used to calibrate Z_{DR} and Z_H of BSL. The Z_H measured from PSN were then corrected by using calibrated Z_H of BSL using self-consistency method and Z_H measured by PARSIVEL. The gage rainfall data were used to assess the performance of three Z_H bias correction methods for PSN which is SPOL.

The accuracy of rainfall estimation using corrected reflectivity was evaluated to measure the effectiveness of each method for calculating the difference reflectivity between PSN and BSL (PARSIVEL). Two rainfall events were used, occurring on 25 August 2014 and 8 September 2012 (Table 1). The August and September events were caused by low pressure systems over southern and northern Korea, respectively.

Figure 2 shows the time series of Z_H observed from BSL radar on 8 September in 2012 and 25 August in 2014. The precipitation within radar coverage on 8 September in 2012 was occurred by low pressure with the front located at northern part of Korea. The core of the precipitation systems was elongated from south to north and moved to eastward. The maximum reflectivity of the core was more than 45 dBZ and caused rainfall at the western part of radar center at 0300 LST (Fig. 2(a)), became more organized shape at the eastern part of radar center at 0400 LST (Fig. 2(c)), and moved to eastward and located out of land at 0500 LST (Fig. 2(e)) on 8 September in 2012. The precipitation system on 25 August in 2014 was caused by the low pressure located at southern part of Korea. The two strong rainfall within the radar coverage were located at south-western part of radar center with distance between 120 km and 150 km and southern part of radar center with distance between 30 km and 90 km, respectively at 1200 LST on 25 August in 2014 (Fig. 2(b)). The two convective cells moved to eastward, their strength were intensified and the area of rainfall was wider at 1300 LST (Fig. 2(d)). The two systems moved to eastward continuously, were merged together at 1400 LST (Fig. 2(f)).

Figure 3 shows the time series of hourly rainfall and daily accumulation measured by a gage which recorded highest daily rainfall within radar coverage on 8 September in 2012 and 25 August in 2014. The highest daily accumulated rainfall was recorded from North Changwon (ID 255) and Geumjeong (ID 939) on each day, respectively. The daily accumulation of ID 255 was 150 mm, the maximum hourly rainfall was around 40 mm, and the duration of the rainfall was 7 hours (Fig. 3(a)). The daily accumulation of ID 939 was around 270 mm, the maximum hourly rainfall was more than 100 mm h^{-1}. The rainfall amount for 3 hours (1000 LST, 1400 LST, and 1500 LST) were mainly contributed to the total rainfall accumulation on 25 August in 2014 (Fig. 3(b)).

3 Methodology

3.1 Z and Z_{DR} bias correction for BSL

Before calculating reflectivity bias for PSN using BSL, Z_H and Z_{DR} must be corrected for bias. Z_{DR} bias correction is important for the absolute calibration of the radar using a self-consistency method. Gorgucci et al. (1999) proposed using a vertical pointing scan of light rain, to take advantage of the nearly spherical shape of the raindrops as seen from below. Ryzhkov et al (2005) used the elevation angle dependency of Z_{DR} as an alternative technique and concluded that the high variability of Z_{DR} in rainfall prohibited the method from achieving the required

absolute calibration accuracy of 0.2 dB. They instead proposed a method that utilizes the structural characteristics of the melting layer in stratiform clouds and the dry aggregated snow present above the melting layer. Z_{DR} measurements from dry aggregated snow above the melting layer resulted in a mean S-band value of 0.2 dB and an accuracy of 0.1–0.2 dB. Trabal et al. (2009) evaluated two methods using the intrinsic properties of dry aggregated snow present above the melting layer and light rain measurements close to the ground, and found that a Z_{DR} calibration accuracy of 0.2 dB or better was achieved using either method.

Vertical pointing data were not available in the present case, and the scan strategy, with six elevation angles, was unable to detect the melting layer. Therefore, in this study, light rain measurements close to the ground were used to calibrate Z_{DR}. Light rain was defined using a threshold of 20 dBZ $\leq$ Z $\leq$ 28 dBZ, as proposed by Marks et al. (2011). The assumption of Z_{DR} is close to zero in case of the small rain drop like drizzle was chosen for this study. The Z_{DR} observed from BSL having with reflectivity in the range of 20 dBZ to 28 dBZ for given time period were averaged. Then the averaged Z_{DR} was taken as a Z_{DR} bias.

The Z_H bias was calculated by self-consistency method using a 9-gate moving average of bias corrected Z_{DR} in the range of 0.2 dB to 3.0 dB to improve the accuracy. This method depends on the notion that Z_H, Z_{DR}, and K_{DP} are independent in rain, and that Z_H can be estimated from Z_{DR} and K_{DP}. The difference between the computed and observed values of Z_H is referred to as the Z bias. Following the method of Ryzhkov et al. (2005), the entire spatial and temporal domain was divided into 1 dB intervals of Z_H between Zmin (30 dBZ) and Zmax (50 dBZ), and the $K_{DP}(Z_H)$ and $Z_{DR}(Z_H)$ within each interval were calculated. The Z_H bias is then determined by matching the integrals:

$$I_1 = \sum_{Z_{\min}}^{Z_{\max}} K_{DP}(Z) n(Z) \Delta Z , \quad (1)$$

$$I_2 = \sum_{Z_{\min}}^{Z_{\max}} 10^{0.1 Z_m} f(Z_{DR}) n(Z) \Delta Z , \quad (2)$$

The function of $f(Z_{DR})$ in Eq. (2) can be well approximated by a fourth-order polynomial fit for certain range of Z_{DR} (Gourley et al., 2009) like Eq. (3).

$$f(Z_{DR}) = 10^{-5}(a_0 + a_1 Z_{DR} + a_2 Z_{DR}^2 + a_3 Z_{DR}^3) , \quad (3)$$

The estimated Z_H bias is determined from Vivekanandan et al. (2003) by

$$Z_H bias(dB) = 10\log(\frac{I_2}{I_1}), \quad (4)$$

If the radar is well calibrated, Z_H bias should be equal to 0. The coefficients of $f(Z_{DR})$ were calculated by T-matrix scattering method using long period DSD data and are 4.26, -4.67, 2.67, and -0.54, respectively.

3.2 Equidistance line method

To calculate the reflectivity bias of PSN, which is single polarization radar, three approaches were used: the equidistance line method, the overlapping area method, and the disdrometer method. The first approach is to compare the reflectivities along the line that is equidistant between the two radars. To determine this line for the two radars, the effective radius was set to 100 km and the distance between the two radars and the azimuthal angle pointing from BSL to PSN were calculated using their latitude and longitude values. The start and end azimuthal angles for comparison of reflectivity were then calculated as follows:

$$AZ_{st} = \beta - a\cos(0.5 \times dr / rc) \quad (5)$$

$$AZ_{end} = \beta - a\cos(0.5 \times dr / rc) + 2 \times a\cos(0.5 \times dr / rc), \quad (6)$$

where AZ_{st} and AZ_{end} are the start and end azimuthal angles for the comparison, respectively; β is an azimuthal angle which is the angle between north and the bearing from BSL points to PSNand *rc* and *dr* are the effective radius and distance from BSL to PSN, respectively. The distance between the two radars is 76.9 km, and the start and end azimuthal angles of BSL (PSN) are 79 (35) and 213 (261) degrees, respectively (Fig. 4).

To compare the reflectivity observed of targets at the almost same height from both radars, the beam height was calculated assuming a standard atmospheric beam propagation (Rinehart, 2010), as follows:

$$H = \sqrt{r^2 + (R'+H_0)^2 + 2r(R'+H_0)\sin\phi} - R', \quad (7)$$

where *r* is the slant range from the radar, Φ is the elevation angle of the radar beam, H_0 is the height of the radar antenna above sea level, and R' = (4/3)R, where R is the Earth's radius (6,371 km). The radar antenna heights of PSN and BSL are 547 and 1085 m, respectively. Figure 5 shows the beam height of PSN with blue solid line and BSL at the equidistance line

(blue dashed line as shown in Fig. 4). EL1 to EL6 show the elevation angles from smallest to largest. The smallest difference in beam height between the two radars is 149 m, which was obtained using the fourth elevation angle of PSN and the third elevation angle of BSL. Therefore, the reflectivity bias of PSN was calculated by averaging the difference of reflectivity along with the equidistance line observed from fourth elevation angle of PSN and third one of BSL.

3.3 Overlapping area method

In the second approach, the overlapping area for the two radars was calculated by matching the coordinates. The polar coordinate of two radars was converted to a Cartesian coordinate with a spatial resolution of 1 km. The overlapping area was then determined by considering the distances between the two radars in the east–west and north–south directions. Figure 6 shows a schematic diagram of the overlapping area for the two radars. The distance between two radars in east-west and north-south direction are 42 km and 64 km, respectively. The reflectivity observed from both radars at the pixels designated at the overlapping area as shown by blue rectangle in right panel of Fig. 6 were compared to calculate the Z_H bias of PSN. The extracted domain of PSN and BSL for the comparison is 158 × 136 km.

3.4 Disdrometer method

The third and final approach is to use DSD observations from the PARSIVEL disdrometer. The reflectivity was calculated from the DSD at 1 min resolution, and averaged over 10 mins to match the radar time resolution. Figure 7 shows a schematic of the procedure used to match the radar and PARSIVEL data. The PARSIVEL disdrometer is located ~9 km from the radar, at an azimuthal angle of 87 degrees. The radar reflectivity was averaged over a domain of 13 gates × 3 degrees in azimuth, centered at the PARSIVEL location. The reflectivity observed by BSL or PARSIVEL subtracted from that observed by PSN was taken as a Z_H bias and it will be applied to all pixels of PSN coverage.

3.5 Validation

The normalized error (NE), root-mean-square error (RMSE), and correlation coefficient (CC) between rainfall estimates and measurements from 121 gauges were calculated to measure the performance of each bias correction method. The rain gages were 0.5 mm tipping-bucket type.

Time resolution of gages is 1 min and data quality control was done by KMA. These quantities are defined as follows:

$$NE = \frac{\frac{1}{N}\sum_{i=1}^{N}\left|R_{R,i} - R_{G,i}\right|}{\overline{R_G}} \quad (8)$$

$$RMSE = \left[\frac{1}{N}\sum_{i=1}^{N}(R_{R,i} - R_{G,i})^2\right]^{1/2} \quad (9)$$

$$CC = \frac{\sum_{i=1}^{N}(R_{R,i} - \overline{R_R})(R_{G,i} - \overline{R_G})}{\left[\sum_{i=1}^{N}(R_{R,i} - \overline{R_R})^2\right]^{1/2}\left[\sum_{i=1}^{N}(R_{G,i} - \overline{R_G})^2\right]^{1/2}}, \quad (10)$$

where N is the number of radar rainfall (R_R) and gauge rainfall (R_G) pairs, and $\overline{R_R}$ and $\overline{R_G}$ are the average hourly rain rates from radar and gauges, respectively. These quantities were calculated using total accumulated rainfall amounts for analyzed time period from radar and gauge measurements at each point. The radar rainfall value at each point was obtained by averaging rainfall over a small area (1 km × 1°) centered on the corresponding rain gauge. The radar rainfall was calculated using the relation $Z = 200\ R^{1.6}$ and $Z = 300\ R^{1.4}$.

4 Results

4.1 Equidistance line method

Before estimating radar rainfall rates, reflectivity biases were calculated using each of the three methods. Figure 8 shows time series of the average reflectivity difference between PSN and BSL at the equidistance line and the number of samples used in each calculation, on 25 August 2014. The average difference over the entire time period was –7.85 dB, and the largest difference was –12.46 dB. It means that the reflectivity observed by PSN was underestimated comparing with BSL. The number of samples used for each calculation was determined using a beam height difference threshold of 0.1 km. The number of samples was generally above 60, but it was smaller than 60 after 1450 LST. The dominant peak of the averaged reflectivity difference occurred from 1500 LST would be caused by the decreased sample number for the

comparison of reflectivity observed from both radars. Figure 9 shows the same information for 8 September 2012. The average reflectivity difference over the entire time period was – 2.56 dB, and the largest difference was –6.77 dB. The number of samples was less than 50 until 0310 LST, after which it increased to more than 50. This result suggests that the rainfall observed from both BSL and PSN radar was not located enough over the equidistance line to get a reliable comparison until 0310 LST.

Figure 10 shows the scatter plot of total accumulated radar rainfall amount for analyzed time period, calculated using $Z = 200R^{1.6}$ and $Z=300R^{1.4}$ and gauge rainfall, for 25 August 2014 and 8 September 2012. The RMSE, NE, and CC of rainfall pairs for $Z = 200R^{1.6}$ ($Z=300R^{1.4}$) on 25 August 2014 were improved from 65.7 (66.1) to 32.6 (27.0) mm, from 0.79 (0.81) to 0.36 (0.31), and from 0.88 (0.87) to 0.89 (0.88), respectively. On 8 September 2012, the RMSE, NE, and CC for $Z = 200R^{1.6}$ ($Z=300R^{1.4}$) changed from 30.0 (28.5) to 22.5 (20.0) mm, from 0.58 (0.56) to 0.41 (0.36), and from 0.81 (0.8) to 0.78 (0.76), respectively, by the use of bias correction. In both cases, the use of corrected reflectivity for rainfall estimation resulted in much better accuracy than did using raw reflectivity.

4.2 Overlapping area method

Figure 11 shows time series of the mean reflectivity differences between PSN and BSL in the overlapping area, and the number of samples used for calculation of Z_H bias on 25 August 2014. Bias values ranged from –11.7 to –8.3 dB over the period analyzed. The bias was stable until 1440 LST, after which it fluctuated as the number of samples decreased. Figure 12 shows the same information for 8 September 2012. Bias values ranged from –4.66 to 0.22 dB, and lower bias values were occurred from 0300 LST to 0400 LST. The fluctuation also would be caused by the sudden change of microphysical characteristics of rainfall pass through the overlapping area for both radars. It would reduce the accuracy of Z_H of BSL corrected by self-consistency. The radar rainfall estimation was done by using observed and corrected Z_H as an input of Z-R relations.

Figure 13 shows a scatter plot of total accumulated radar rainfall amount for entire analyzed time period, calculated using $Z = 200\ R^{1.6}$ and $Z=300R^{1.4}$ and gauge rainfall, for 25 August 2014 and 8 September 2012. The RMSE and NE of rainfall pairs for $Z = 200R^{1.6}$ ($Z=300R^{1.4}$) on 25 August 2014 were improved from 65.7 (66.1) to 29.7 (25.8) mm and from 0.79 (0.81) to 0.31 (0.28), respectively. On 8 September 2012, RMSE and NE for $Z = 200R^{1.6}$ ($Z=300R^{1.4}$)

were improved from 30.0 (28.5) to 21.8 (19.1) mm and from 0.58 (0.56) to 0.40 (0.34), respectively, by the use of bias correction, while CC for $Z=200R^{1.6}$ was unchanged at 0.81 and that of $Z=300R^{1.4}$ were changed 0.8 to 0.79. Again, in both cases the use of corrected reflectivity for rainfall estimation was found to improve the accuracy compared with raw reflectivity.

4.3 Disdrometer method

Before using the disdrometer bias correction method to estimate rainfall rates, 10 min rain rates obtained directly from DSDs and from collocated gauges were compared. Figure 14 shows the time series of rain rate obtained by PARSIVEL and collocated gauges on 25 August 2014. Daily total rainfall amounts for PARSIVEL and the gauges were 129.4 and 116.0 mm, respectively. The difference in the totals is only 13.4 mm, and the RMSE and CC between the 10 min time series were 0.52 mm h^{-1} and 0.99, respectively. On 8 September 2012 (not shown), daily total rainfall amounts for PARSIVEL and the gauge were 54.4 and 55.0 mm, respectively. The difference between the total daily rainfall amounts was 0.7 mm and the RMSE and CC between the two 10 min series were 0.62 mm h^{-1} and 0.96, respectively. It is concluded that DSDs were sufficiently reliable to use as a reference with which to calculate the radar bias.

Figure 15 shows time series of reflectivity obtained by radar and by PARSIVEL, and the radar bias, on 25 August 2014. The bias was more stable before 1200 LST than after 1500 LST. PARSIVEL reflectivity fell to zero from 1230 to 1340 LST because the precipitation system moved away from the PARSIVEL site. The sudden change of rainfall would cause the unstable reflectivity difference from 1340 LST to 1500 LST. The threshold of reflectivity value observed from both PSN and PSRSIVEL should be considered for the comparison to get more reliable Z_H bias. The bias would be obtained more accurately when the reflectivity values observed from both instruments were higher than 15 dBZ in this event. Because of this discontinuity, the bias can be considered to be reliable only until 1200 LST. The bias values ranged from -13.4 to -3.1 dB until 1200 LST. Figure 16 shows time series of reflectivity obtained by radar and by PARSIVEL, and the radar bias on 8 September 2012. On this occasion there was no reflectivity data from either PARSIVEL or radar until 0330 LST. The bias values were distributed from -14.3 to 12.7dB.

Figure 17 shows a scatter plot of total accumulated radar rainfall amount for the entire time period, calculated using $Z = 200R^{1.6}$ and $Z=300R^{1.4}$ and gauge rainfall, on 25 August 2014 and 8 September 2012. The RMSE and NE of rainfall pairs for $Z = 200R^{1.6}$ ($Z=300R^{1.4}$) on 25

August 2014 were improved from 65.7 (66.1) mm to 42.0 (61.4) mm and from 0.79 (0.81) to 0.40 (0.53), respectively. On 8 September 2012, RMSE and NE for $Z = 200R^{1.6}$ ($Z=300R^{1.4}$) decreased from 30.1 (28.6) to 24.6 (23.9) mm, and from 0.58 (0.56) to 0.46 (0.44), respectively, while CC for $Z = 200R^{1.6}$ ($Z=300R^{1.4}$) decreased from 0.81 (0.8) to 0.65 (0.59). In both cases, using corrected rather than raw reflectivity for rainfall estimation improved accuracy as measured by RMSE and NE, but reduced accuracy as measured by CC.

4.4 Discussion

Figure 18 shows RMSE of total rainfall amount for entire time period obtained by gage and $Z=200R^{1.6}$ from each of the different bias correction methods on 25 August 2014 and 8 September 2012. Red, black, green, and blue bars show the RMSE obtained using the uncorrected, equidistance line, overlapping area, and disdrometer methods, respectively. The disdrometer method produced the lowest RMSE before 1200 LST and the highest RMSE after 1200 LST (Fig. 18(a)). This behavior can be attributed to the varying stability of the reflectivity calculated by PARSIVEL (Fig. 15). The overlapping method is more accurate than the equidistance line method for the entire time period, except at 1400 LST. All the bias correction methods performed better than the uncorrected method, except for the period during which DSDs were unavailable. On 8 September 2012, the RMSE of the overlapping area method was lower than that of the other methods for the entire period, except at 0500 and 0600 LST (Fig. 18(b)). The disdrometer method produced lower RMSE at 0600 LST, when DSDs were available, and the equidistance line method was more accurate at 0500 LST, when the sample number was high (Fig. 15). Comparing the RMSE between two events, the large fluctuation was occurred. It would be caused by the difference of total rainfall amount between two rainfall systems. The maximum total rainfall amount for both cases were around 250 mm for 25 August and 150 mm for 8 September 2012. Another reason of the fluctuation would be the difference of radar hardware calibration error for PSN between two events.

Considering the entire period covering both events, the overlapping area method showed the best performance, as measured by RMSE. The accuracy of radar rainfall estimates could be improved by combining the three approaches, using metrics such as DSD temporal stability and the number of samples available for the equidistance line method to select the best method for a particular situation. It is worth to noting that the result would be changed when the drop size distributions was fluctuated with height especially at the layer between radar beam and ground in case of disdrometer method.

5 Conclusions

Three methods for determining the reflectivity bias of single polarization radar using dual polarization radar reflectivity and disdrometer data were proposed and examined for two rainfall events caused by low pressure over the Korean Peninsula on 25 August 2014 and 8 September 2012. Single polarization radar reflectivity was underestimated by more than 12 dB and 7 dB during the August and September events, respectively. All three methods improved the accuracy of estimated rainfall, except during a period when DSDs were not observed (as the precipitation system did not pass over the disdrometer location).

The rainfall estimation using $Z = 200R^{1.6}$ and $Z=300R^{1.4}$ and gauge rainfall were examined for 25 August 2014 and 8 September 2012 to investigate the accuracy of each method. The RMSE, NE, and CC of rainfall pairs for $Z = 200R^{1.6}$ ($Z=300R^{1.4}$) on 25 August 2014 in case of using equidistance method were improved from 65.7 (66.1) to 32.6 (27.0) mm, from 0.79 (0.81) to 0.36 (0.31), and from 0.88 (0.87) to 0.89 (0.88), respectively. On 8 September 2012, the RMSE, NE, and CC for $Z = 200R^{1.6}$ ($Z=300R^{1.4}$) changed from 30.0 (28.5) to 22.5 (20.0) mm, from 0.58 (0.56) to 0.41 (0.36), and from 0.81 (0.8) to 0.78 (0.76), respectively.

The RMSE and NE of rainfall pairs for $Z = 200R^{1.6}$ ($Z=300R^{1.4}$) on 25 August 2014 in case of using overlapping method were improved from 65.7 (66.1) to 29.7 (25.8) mm and from 0.79 (0.81) to 0.31 (0.28), respectively. On 8 September 2012, RMSE and NE for $Z = 200R^{1.6}$ ($Z=300R^{1.4}$) were improved from 30.0 (28.5) to 21.8 (19.1) mm and from 0.58 (0.56) to 0.40 (0.34), respectively, by the use of bias correction, while CC for $Z=200R^{1.6}$ was unchanged at 0.81 and that of $Z=300R^{1.4}$ were changed 0.8 to 0.79.

The RMSE and NE of rainfall pairs for $Z = 200R^{1.6}$ ($Z=300R^{1.4}$) on 25 August 2014 in case of using disdrometer method were improved from 65.7 (66.1) mm to 42.0 (61.4) mm and from 0.79 (0.81) to 0.40 (0.53), respectively. On 8 September 2012, RMSE and NE for $Z = 200R^{1.6}$ ($Z=300R^{1.4}$) decreased from 30.1 (28.6) to 24.6 (23.9) mm, and from 0.58 (0.56) to 0.46 (0.44), respectively, while CC for $Z = 200\ R^{1.6}$ ($Z=300R^{1.4}$) decreased from 0.81 (0.8) to 0.65 (0.59).

The use of these bias correction methods reduced rainfall RMSE by up to 50%. Overall, the accuracy of rainfall estimation was highest when the overlapping area method was used to correct radar reflectivity.

The reflectivity biases obtained using the disdrometer and equidistance line methods were more temporally variable than those obtained using the overlapping area method. There were several

hours during which the disdrometer method was more accurate than the overlapping area method. We suggest that combining the overlapping area method with the disdrometer method, using threshold criteria such as the temporal stability of reflectivity and the number of samples available would allow more accurate estimates of rainfall. However, optimum values for the domain size for the overlapping area method, the sample number threshold for the equidistance line method, and the reflectivity threshold for the disdrometer method should be determined in order to combine the three methods most effectively.

Acknowledgements

The authors thank the Ministry of Land, Infrastructure, and Transport of the Korean government and the Korean Meteorological Administration for providing radar data and AWS (Automatic Weather System) gauge data. This research was funded by the Korea Meteorological Industry Promotion Agency under Grant KMIPA 2015-1050. And this research was partly funded by the Korea Meteorological Industry Promotion Agency under Grant KMIPA 2015-1060

References

Austin, P. M.: Relation between measure radar reflectivity and surface rainfall, Monthly Weather Review, 115, 1053-1070, 1987.

Battan, L. J.: Radar Observations of the Atmosphere, The University of Chicago Press, Chicago and London, 324, 1973.

Campos, E. and Zawadzki, I.: "Instrumental uncertainties in Z-R relations", Journal of Applied Meteorology, 36, 1088-1102, 2000.

Gorgucci E., Scarchilli G., and Chandrasekar V.: Calibration of radars using polarimetric techniques. IEEE Transactions on Geoscience and Remote Sensing, 30: 853-858, 1992.

Gorgucci, E., Scarchilli, G., and Chandrasekar, V.: A procedure to calibrate multiparameter weather radar using properties of the rain medium. IEEE Transactions on Geoscience and Remote Sensing, 37: 269–276, 1999.

Goddard J, Tan J, and Thurai M.: Technique for calibration of meteorological radars using differential phase. Electronic Letters, 30: 166 – 167, 1994.

Jang, M., Lee, D., and You, C.: Z-R relationship and DSD analyses using a POSS disdrometer. Part I: Precipitation cases in Busan, Journal of the Korean Meteorological Society, 40, 557-570, 2004.

Loffler-Mang, M. and Joss, J.: An optical disdrometer for measuring size and velocity of hydrometeors, J. Atmos. Oceanic. Technol., 17, 130-139, 2000.

Marks, D. A., Wolff, D. B., Carey, L. D., and Tokay, A.: Quality control and calibration of the dual-polarization radar at Kwajalein, RMI. Journal of Atmospheric and Oceanic Technology, 28: 181–196, 2011.

Rinehart, R. E.: Radar for meteorologists, fifth edition, Rinehart Publications, Nevada, United States, pp. 482, 2010.

Ryzhkov, A. V., Giangrande, S. E., Melnikov, V. M., and Schuur, T. J.: Calibration issues of dual-polarization radar measurements. Journal of Atmospheric and Oceanic Technology, 22: 1138–1155, 2005.

Scarchilli G., Gorgucci E., Chandrasekar V., and Dobaie A.: Self-consistency of polarization diversity measurement of rainfall. IEEE Transactions on Geoscience and Remote Sensing, 34: 22–26, 1996.

Trabal J. M., Chandrasekar V., Gorgucci, E. and McLaughlin D. J.: Differential reflectivity (ZDR) calibration for CASA radar network using properties of the observed medium, Geoscience and Remote Sensing Symposium,2009 IEEE International,IGARSS 2009 (Volume:2) II-960-II963, 2009.

Vivekanandan J, Zrnic D. S., Ellis S. M., Oye R., Ryzhkov A. V., and Straka J.: Cloud microphysics retrieval using S-band dual-polarization radar measurements. Bulletin of the American Meteorological Society, 80(3): 381-388, 1999.

Wilson, J. W. and Brandes, E. A.: Radar measurement of rainfall-A summary, Bulletin of the American Meteorological Society, 60, 1048-1058, 1979.

You, C., Lee, D., Jang, M., Seo, K., Kim, K., and Kim, B.: The characteristics of rain drop size distributions using a POSS in Busan area, Journal of the Korean Meteorological Society, 40, 713-724, 2004.

You, C., Lee, D., Jang, M., Uyeda, H., Shinoda, T., and Kobayashi, F.,: Characteristics of rainfall systems accompanied with Changma front at Chujado in Korea, Asia-Pacific Journal of Atmospheric Sciences, 46, 41-51, 2010.

You, C.-H., Lee, D.-I., and Kang, M.-Y.: Rainfall estimation using specific differential phase for the first operational polarimetric radar in Korea, Advances in Meteorology, vol. 2014, Article ID 41317, 10 pages, doi:10.1155/2014/413717, 2014.

You, C.-H. and Lee, D.-I.: Decadal variation in raindrop size distributions in Busan, Korea, Advances in Meteorology, vol. 2015, Article ID 329327, 8 pages, 2015, doi:10.1155/2015/329327, 2015.

Zhang, J., Wang S., Clarke B.: WSR-88D reflectivity quality control using horizontal and vertical reflectivity structure. Preprints, 11th Conf. on Aviation, Range and Aerospace Meteorology, Hyannis, MA, Amer. Metoer. Soc, CD-ROM, P5.4, 2004

1 Table 1. Rainfall events used for the analysis.

Date	Source	Period of analysis
8 September 2012	Low pressure	0000 LST to 0600 LST
25 August 2014	Low pressure	0900 LST to 1600 LST

2

3

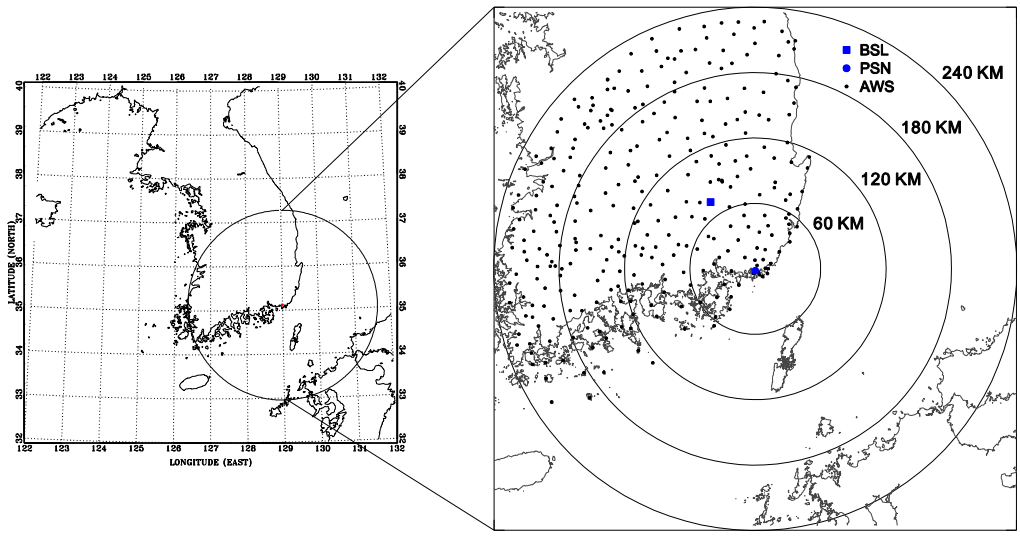

Figure 1. Location of the Bislsan radar (solid rectangle), the PARSIVEL disdrometer and Gudeok radar (solid circle), and rain gauges (black dots) distributed within 240 km of radar coverage. Circles indicate distance from the Gudeok radar, and are drawn at intervals of 60 km.

(a) (b)

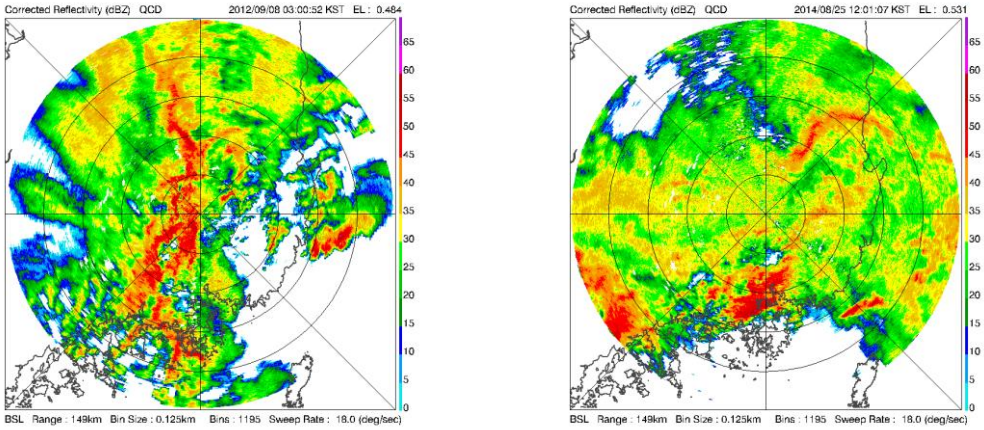

(c) (d)

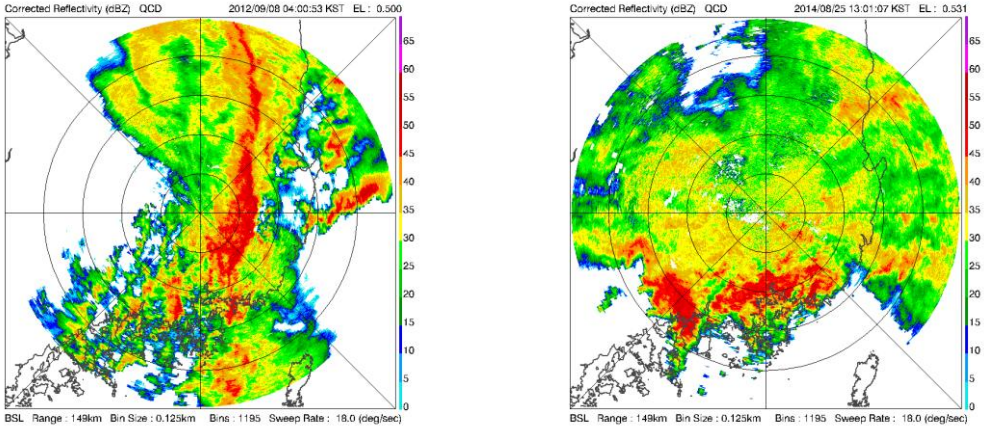

(e) (f)

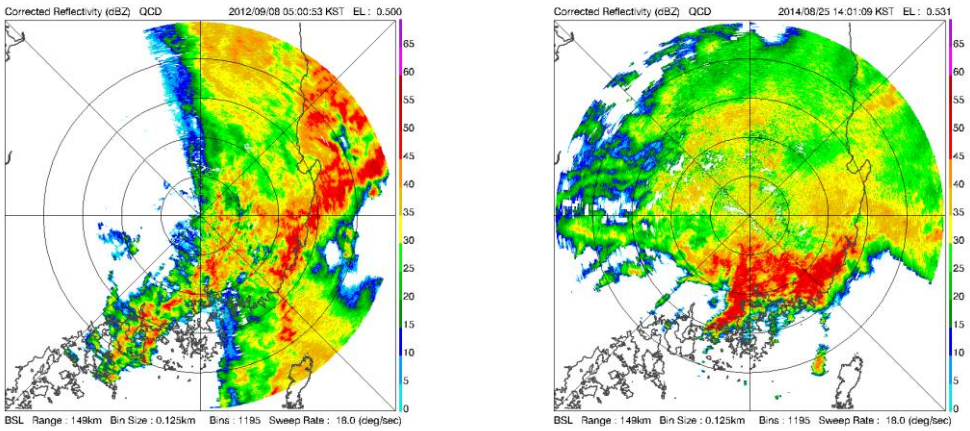

Figure 2. Time series of horizontal reflectivity (ZH) at 0.5 elevation angle observed from BSL (a) 0400 LT, (c) 0500 LT, (e) 0600 LT on 8 September in 2012, (b) 1200 LT, (d) 1300 LT, (f) 1400 LT on 25 August in 2014.

(a)

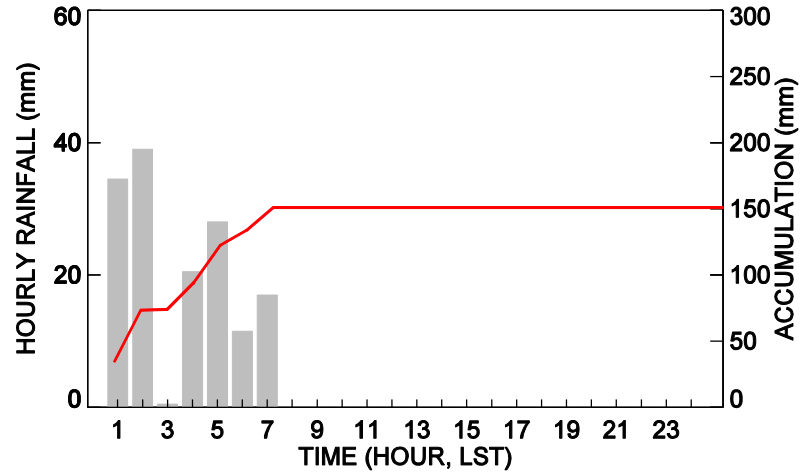

(b)

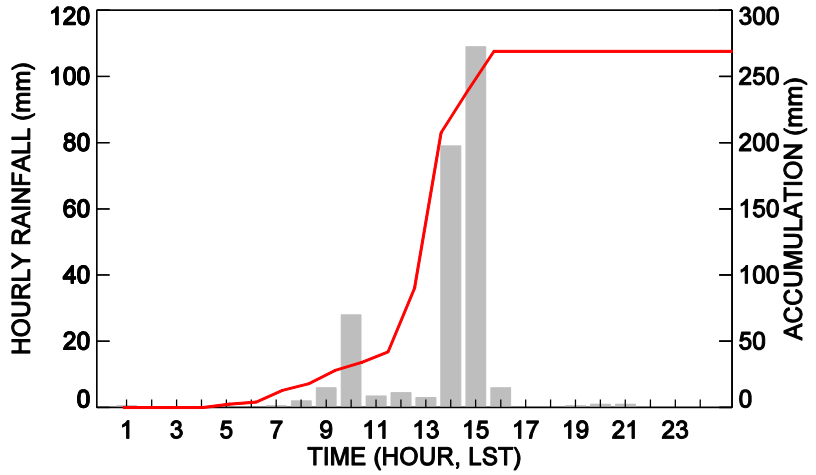

Figure 3. Time series of 1 hour rainfall (bar) and daily accumulated (red line) measured from a gage which recorded highest daily rainfall within radar coverage at (a) North Changwon (ID 255) on 8 September in 2012 and (b) Geumjeong (ID 939) on 25 August in 2014.

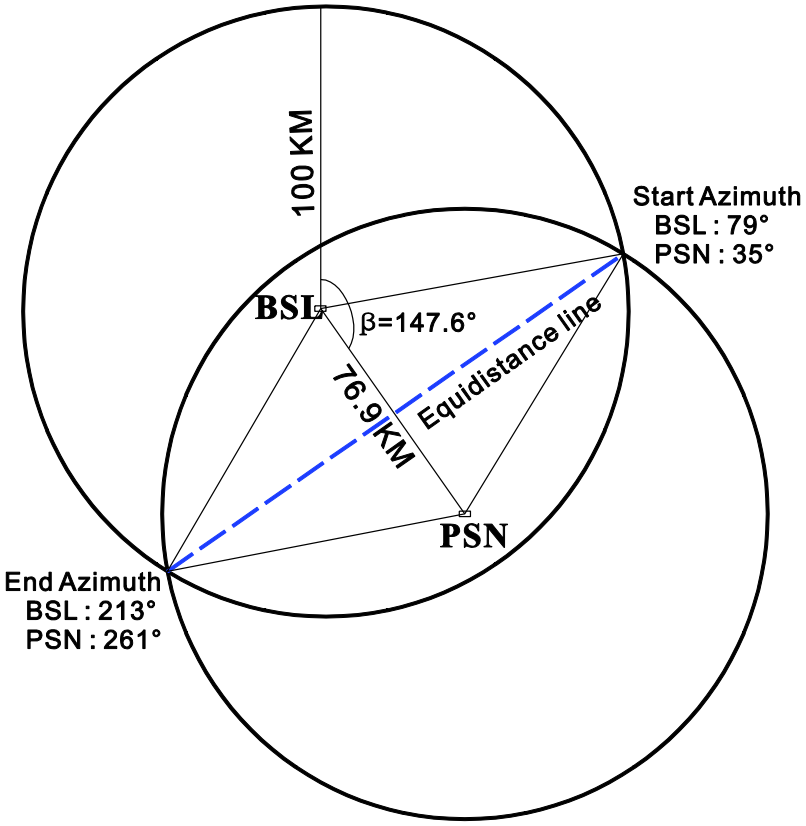

Figure 4. Schematic diagram showing the method used to calculate the line of equidistance between two radars. The effective radius was set to 100 km and the distance between radars is 76.9 km. The azimuthal angle from BSL to PSN is 147.6 degrees. The start and end azimuthal angles are 79 (35) and 213 (261) degrees for BSL (PSN), respectively. The blue dashed line shows the equidistance line.

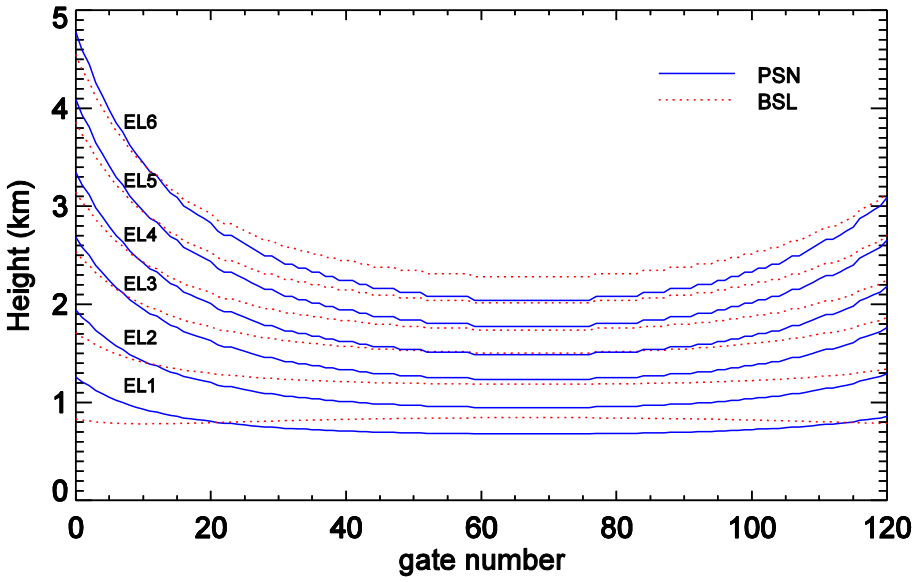

Figure 5. Beam height of PSN (blue solid lines) and BSL (red dotted lines) at the equidistance line. EL1 to EL6 show the lowest, second, third, fourth, fifth, and sixth elevation angles, respectively.

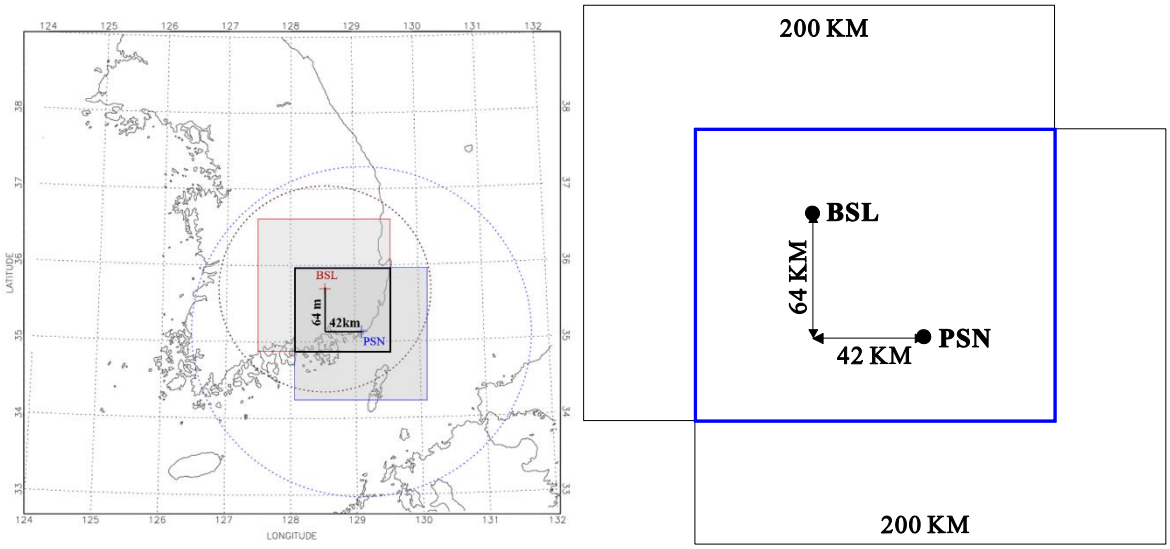

Figure 6. Schematic diagram of the overlapping area for BSL and PSN. The east–west and north–south distances between the two radars are 42 km and 64 km, respectively. The red (blue) dotted circle shows the maximum range of BSL (PSN) and gray shaded area show 200 km by 200 km extracted from each radar coverage in the left panel.

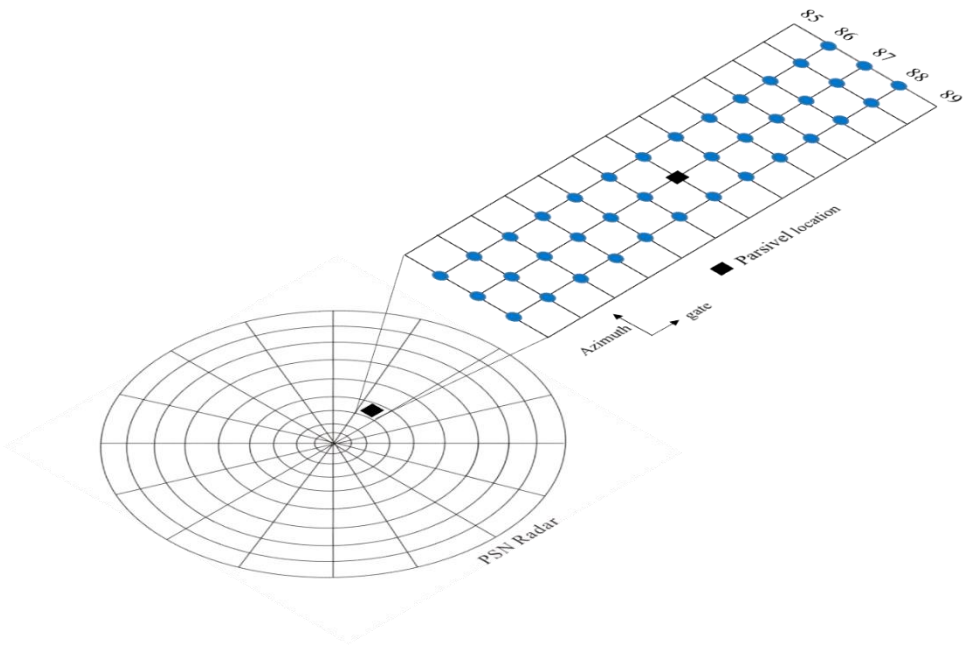

Figure 7. Schematic diagram showing matching of the radar gate and the PARSIVEL disdrometer. PARSIVEL is located ~9 km from the radar, at an azimuthal angle of 87 degrees. The radar reflectivity was averaged over a 3 km × 3° domain centered at the PARSIVEL location.

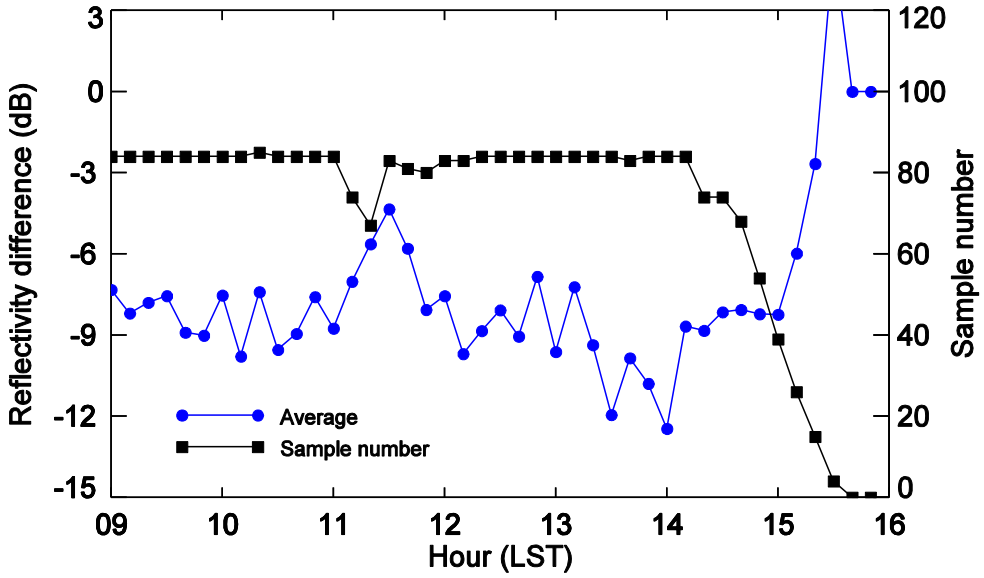

Figure 8. Time series of the average reflectivity difference between PSN and BSL at the equidistance line (blue circles) and the number of samples used in each calculation (black squares) on 25 August in 2014.

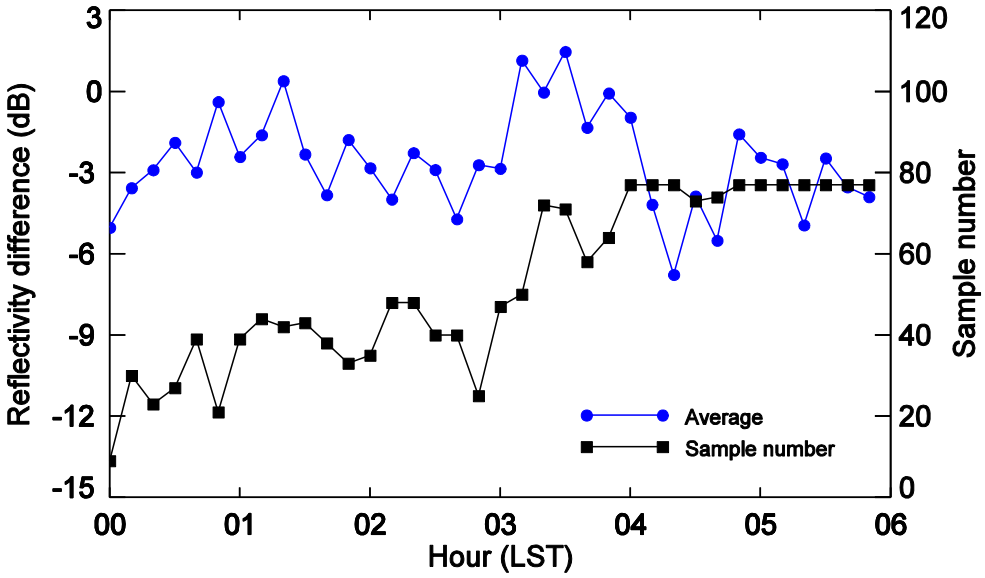

Figure 9. As for Fig. 8 but for 8 September 2012.

(a) (b)

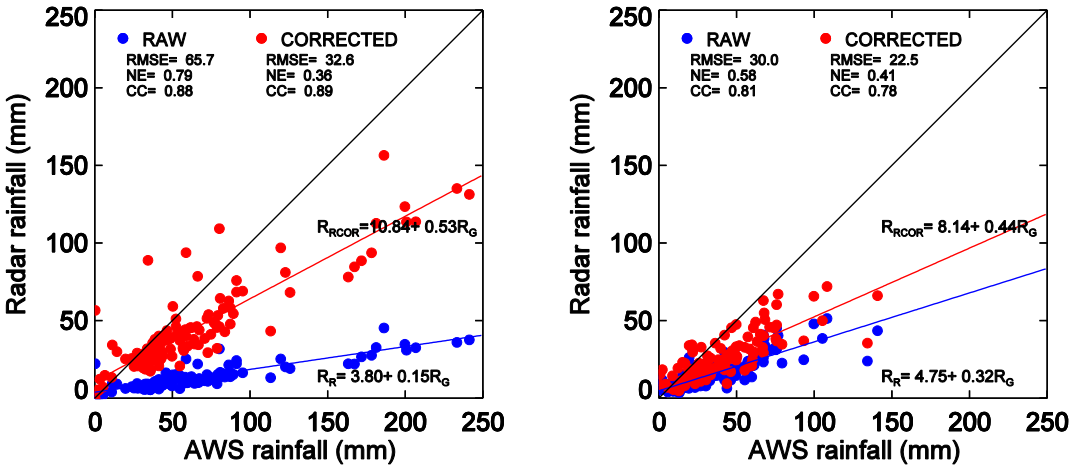

(c) (d)

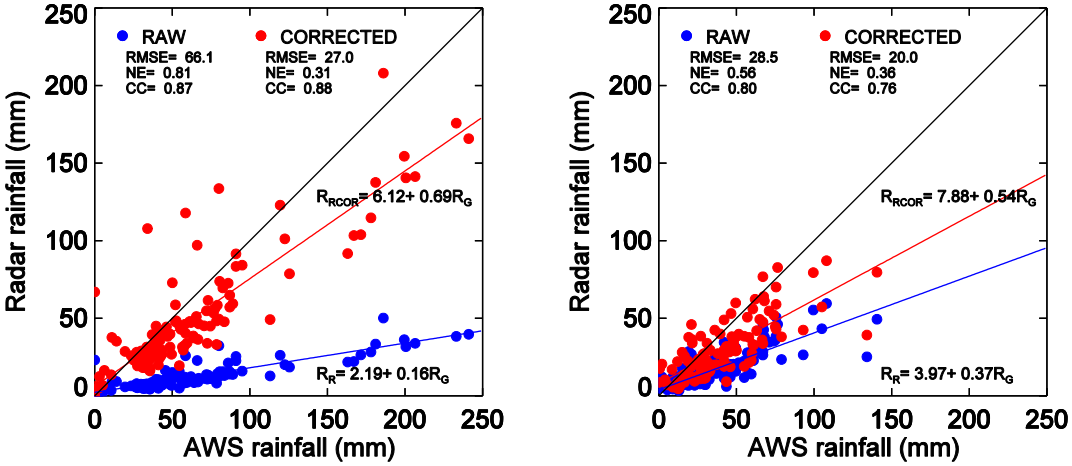

Figure 10. Scatter plot of total accumulated rainfall for analyzed time period calculated by gage and radar using (a and b) $Z = 200\ R^{1.6}$ and (c and d) $Z = 300\ R^{1.4}$ for 25 August 2014 and 8 September 2012, respectively. Blue circles show the rainfall pairs obtained using raw reflectivity and red circles show those obtained using reflectivity corrected with the equidistance line method.

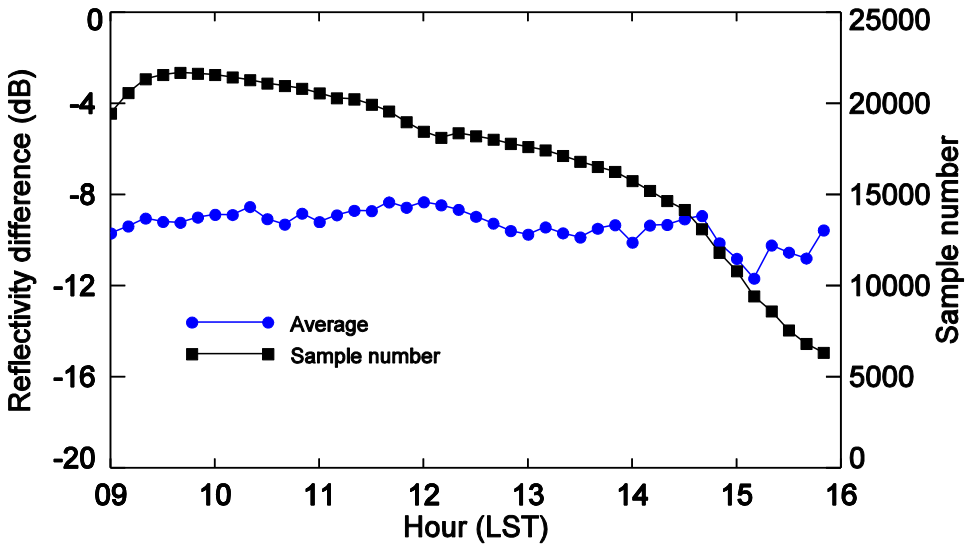

Figure 11. Time series of the average reflectivity difference between PSN and BSL at the overlapping area (blue circles) and the number of samples used in each calculation (black squares) on 25 August in 2014.

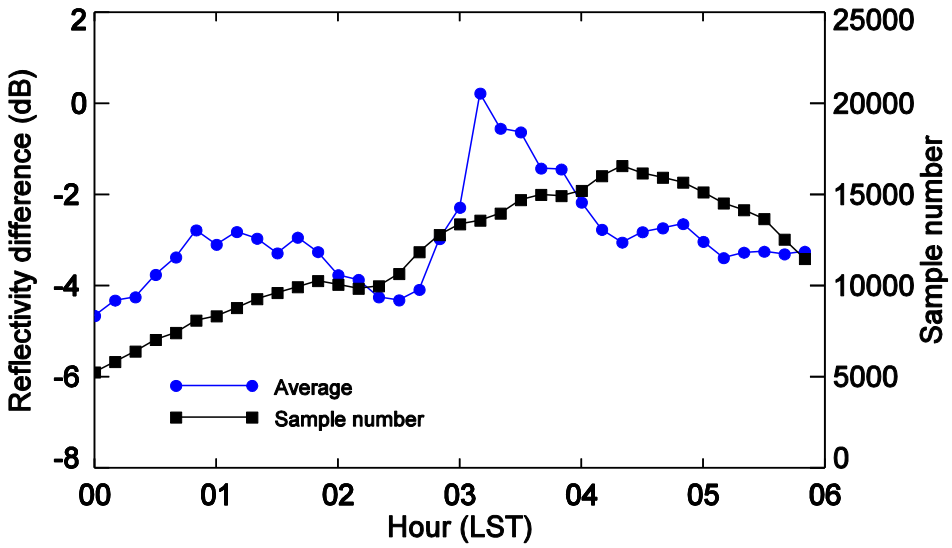

Figure 12. Time series of the average reflectivity difference between PSN and BSL at the overlapping area (blue circles) and the number of samples used in each calculation (black squares) on 8 September in 2012.

1 (a) (b)

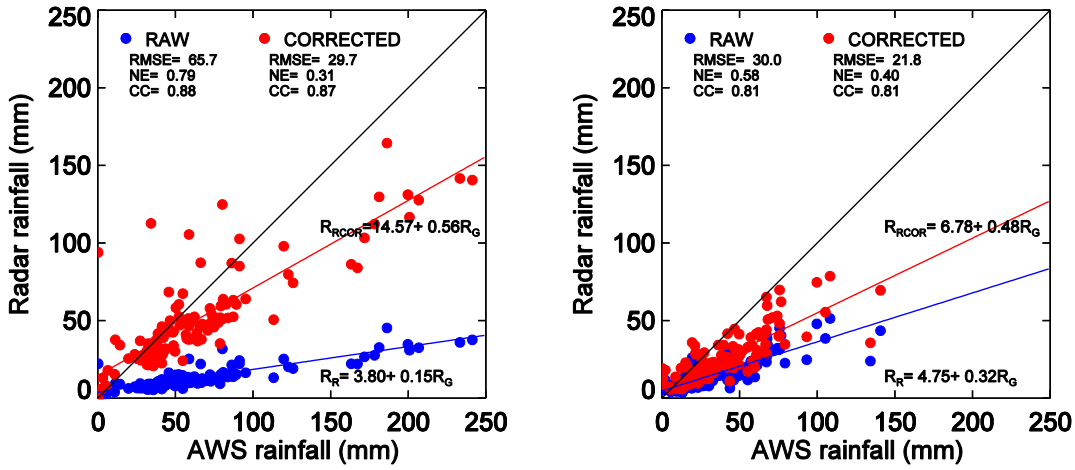

2

3 (c) (d)

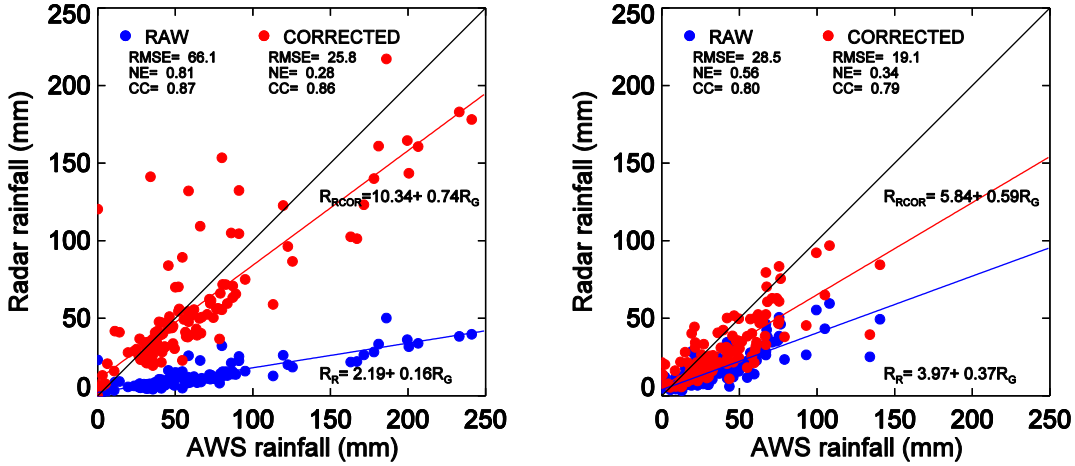

4

5 Figure 13. As for Fig. 10 but for the overlapping area method.

6

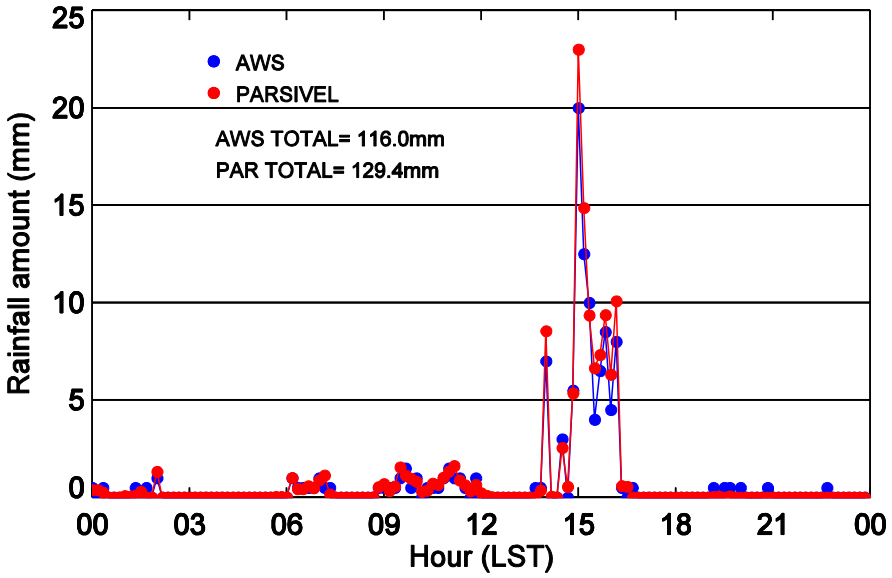

Figure 14. Time series of 10 min rainfall amount as obtained by PARSIVEL (red circles) and collocated gauges (blue circles).

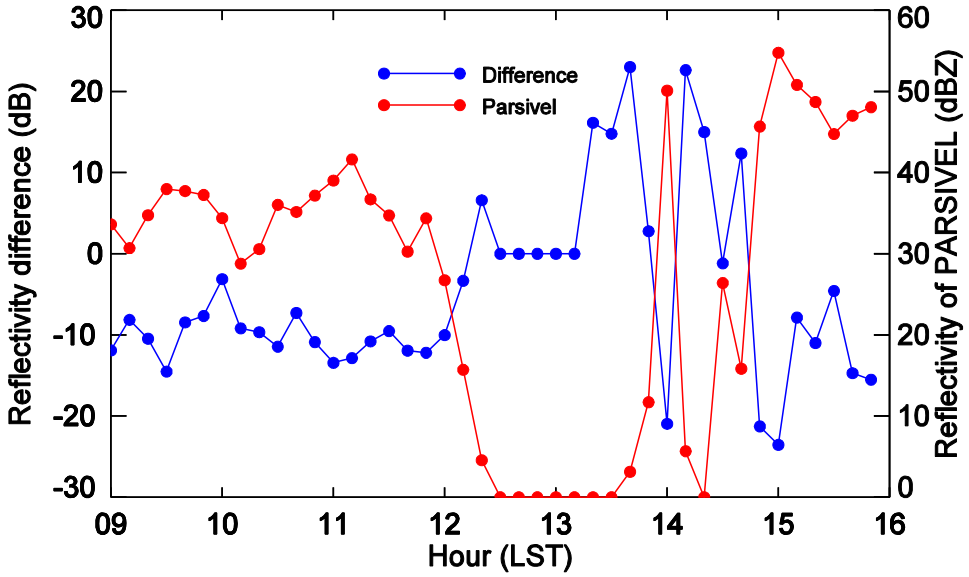

Figure 15. Time series of reflectivity obtained by ~~radar (black circles) and by~~ PARSIVEL (red circles), and the radar bias (blue circles) on 25 August 2014.

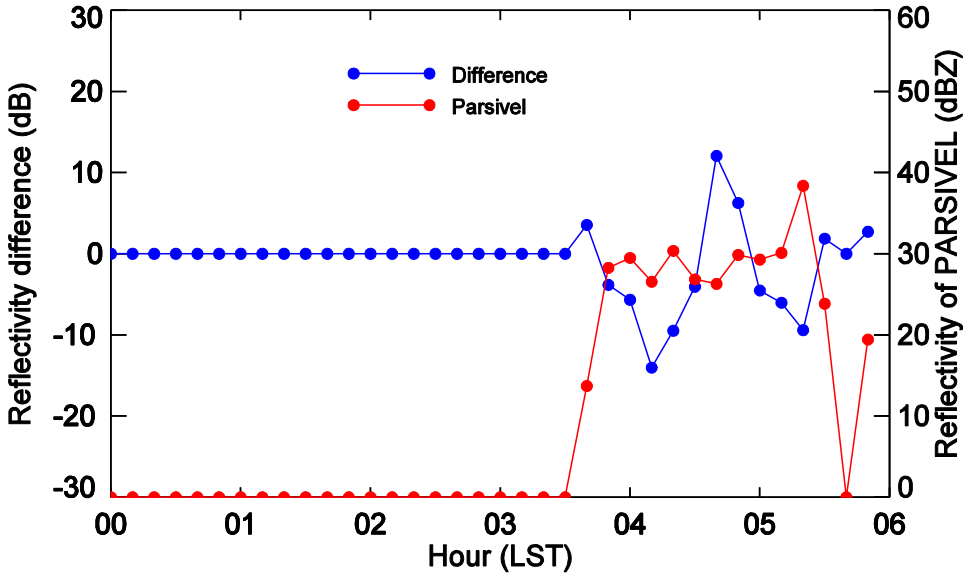

Figure 16. As for Fig. 15 but for 8 September 2012.

1 (a) (b)

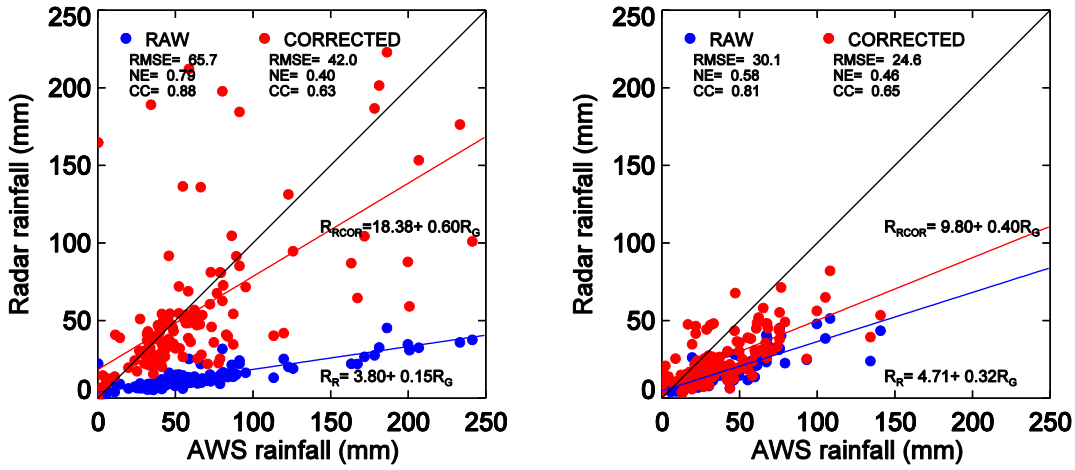

2

3 (c) (d)

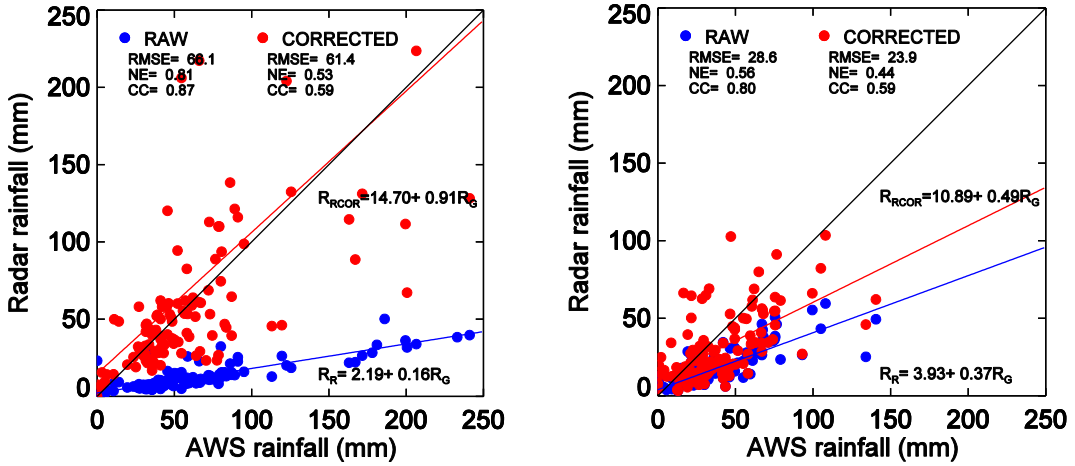

4

5 Figure 17. As for Fig. 10 but for the disdrometer method.

6

(a) (b)

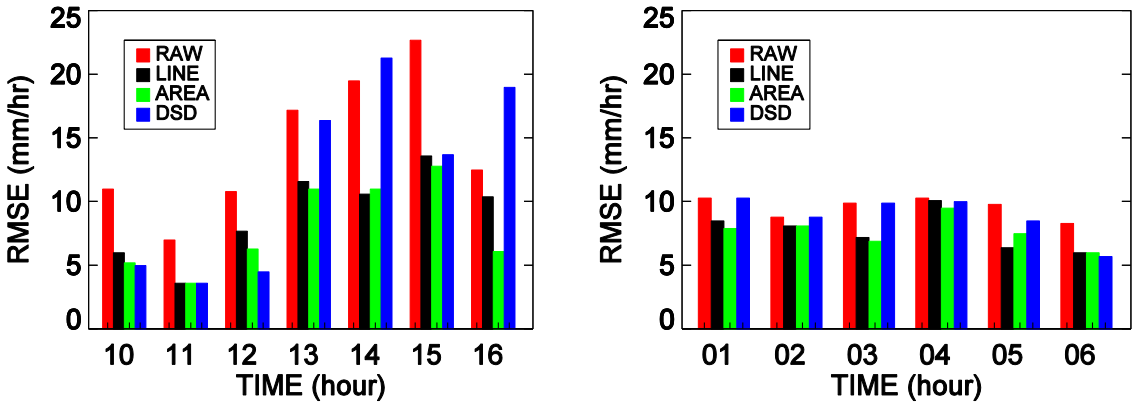

Figure 18. Accumulated rainfall RMSE calculated from radar and gage for different bias correction methods on (a) 25 August 2014 and (b) 8 September 2012. The bars with different colors show results obtained using the raw data, equidistance line method, overlapping area method, and disdrometer method, respectively.